Journal of Cerebral Blood Flow & Metabolism (2012) 32, 2135–2145

www.jcbfm.com

The locus coeruleus-norepinephrine network optimizes coupling of cerebral blood volume with oxygen demand

Lane K Bekar, Helen S Wei and Maiken Nedergaard

Division of Glia Disease and Therapeutics, Center for Translational Neuromedicine, University of Rochester Medical Center, Rochester, New York, USA

Given the brain's uniquely high cell density and tissue oxygen levels bordering on hypoxia, the ability to rapidly and precisely match blood flow to constantly changing patterns in neural activity is an essential feature of cerebrovascular regulation. Locus coeruleus-norepinephrine (LC-NE) projections innervate the cerebral vasculature and can mediate vasoconstriction. However, function of the LC-mediated constriction in blood-flow regulation has never been addressed. Here, using intrinsic optical imaging coupled with an anesthesia regimen that only minimally interferes with LC activity, we show that NE enhances spatial and temporal aspects of functional hyperemia in the mouse somatosensory cortex. Increasing NE levels in the cortex using an α_2-adrenergic receptor antagonist paradoxically *reduces* the extent of functional hyperemia while enhancing the surround blood-flow reduction. However, the NE-mediated vasoconstriction optimizes spatial and temporal focusing of the hyperemic response resulting in a sixfold decrease in the disparity between blood volume and oxygen demand. In addition, NE-mediated vasoconstriction accelerated redistribution to subsequently active regions, enhancing temporal synchronization of blood delivery. These observations show an important role for NE in optimizing neurovascular coupling. As LC neuron loss is prominent in Alzheimer and Parkinson diseases, the diminished ability to couple blood volume to oxygen demand may contribute to their pathogenesis.
Journal of Cerebral Blood Flow & Metabolism (2012) **32,** 2135–2145; doi:10.1038/jcbfm.2012.115; published online 8 August 2012

Keywords: cerebral hemodynamics; intrinsic optical imaging; neurovascular coupling; optical imaging

Introduction

Increases in cerebral blood flow correlate most closely with postsynaptic neural activity, forming the basis for functional magnetic resonance and intrinsic optical imaging techniques (Logothetis, 2007; Raichle and Mintun, 2006). The commonly observed sensory-mediated decrease in surround blood flow, or negative blood oxygenation level-dependent phenomenon seen in functional magnetic resonance imaging has been attributed to an inhibition of neural activity (Devor *et al*, 2007; Shmuel *et al*, 2006). However, the simplest mechanism explaining the surround blood-flow decrease is a vascular-steal phenomenon where local vessel dilation reduces vascular resistance, increasing local flow while reducing flow in the surrounding vascular tree (Harel *et al*, 2002). This is consistent with studies showing decreased surround blood flow despite small increases in surrounding neural activity (Harel *et al*, 2002; Shih *et al*, 2009). Additionally, decreases in blood flow can occur in the face of increased glucose uptake (Devor *et al*, 2008), showing that blood-flow suppression can be driven by metabolism-independent mechanisms.

The locus coeruleus (LC) is a group of electrotonically coupled, unmyelinated, highly branched neurons with extensive varicosities situated along projections throughout the brain designed for volume release of norepinephrine (NE) (Berridge and Waterhouse, 2003). This structure is ideal for simultaneous global NE release in response to salient or noxious stimuli that demand focus/attention (Bekar *et al*, 2008; Hirata and Aston-Jones, 1994). Given the role of catecholamines in peripheral sympathetic control of blood-flow distribution, it is not surprising that NE can affect vessel diameter (Mulligan and MacVicar, 2004; Peppiatt *et al*, 2006) and regulate blood flow in

Correspondence: Professor LK Bekar, Neural Systems and Plasticity Research Group, Department of Pharmacology, University of Saskatchewan, Saskatoon, SK,, Canada S7N 5E5.
E-mail: lane.bekar@usask.ca
This work was supported in part by grants NS075177 and NS078304 from the US National Institutes of Health and National Institute of Neurological Disorders and Stroke to MN, respectively and Canadian Institutes of Health Research postdoctoral fellowship to LKB.
Received 18 April 2012; revised 3 July 2012; accepted 4 July 2012; published online 8 August 2012

the central nervous system (Raichle *et al*, 1975). However, the role that global NE-mediated vasoconstriction plays in functional blood-flow distribution has never been addressed. As prior blood-flow studies are largely performed in deeply anesthetized animals, LC-NE contribution is most certainly inhibited and thus overlooked. We use a model of anesthesia that facilitates the exploration of the LC contribution to functional hyperemia. In this study, we define the impact of LC-NE network activity on sensory-mediated blood-flow distribution kinetics by using intrinsic optical imaging of total and reduced (deoxygenated) hemoglobin as a measure of blood volume and activity-associated oxygen demand, respectively. We show that NE is important for spatially and temporally optimizing blood distribution to active regions. Our data support the idea that coupling of local vasodilation with a global NE-mediated vasoconstriction optimizes blood distribution to active zones.

Materials and methods

Animal Preparation

Animal studies were approved by the University Committee on Animal Resources of the University of Rochester Medical Center and conducted in accordance with NIH guidelines for the care and use of laboratory animals. Male C57Bl6 mice, 8 to 10 weeks of age, were induced with 3% isoflurane and maintained at 1.5% to 2% after intubation and artificial ventilation with a small animal ventilator (SAAR-830; CWE, Ardmore, PA, USA) in series with an isoflurane vaporizer. Depth of anesthesia was monitored by toe-pinch and whisker movement. Body temperature was maintained by a water perfused thermal pad (Gaymar T/Pump, Orchard Park, NY, USA). After establishment of ventilation and stable anesthesia, a femoral artery was cannulated for injection of fluorescein isothiocyanate-dextran and blood gas/blood pressure measurements and a custom-made metal plate was glued to the skull with dental acrylic cement for subsequent mounting on the stage of the imaging microscope. A 3×4 mm region of skull was thinned for intrinsic imaging or removed for multiphoton imaging over the hindlimb and forelimb somatosensory cortices. Agarose (0.8% in saline, 37°C) was applied and a glass coverslip was sealed to the metal plate with dental acrylic cement. For experiments, anesthesia was lightened from 1.5% to 0.5% isoflurane and animals were injected with vecuronium bromide (Norcuron, 0.5 mg/kg intraperitoneally) to aid mechanical ventilation and prevent small reflex movements that could distort imaging. Without vecuronium bromide, animals show a mild paw withdrawal reflex to the properly titrated stimulation (amplitude) paradigm used.

Experimental Treatment

Pretreatment with the selective LC neurotoxin N-(2-chloroethyl)-N-ethyl-2-bromobenzylamine (DSP-4; Sigma, St Louis, MO, USA) (two 50 mg/kg intraperitoneal injections 8 to 10 and 4 to 6 days before experiments) was used to create an LC-norepinephrine-deficient mouse, whereas acute injection of the highly selective α_2-adrenergic antagonist atipamezole (Antisedan, Pfizer, New York, NY, USA; 2 to 3 mg/kg intraperitoneally) was used to potentiate LC-mediated NE release.

High Performance Liquid Chromatography for Cortical Neuromodulator Content

Animals were killed and samples of somatosensory cortex were freshly dissected out and stored at −80°C until analysis. Tissues were sonicated in 10 volumes (wt/vol) of 5% trichloroacetic acid. After centrifugation at 15,000 *g* for 15 minutes at 4°C, 20 μL of supernatant was injected manually into a Rheodyne sample injector (Chelmsford, MA, USA) (with a fixed sample loop of 20 μL) and eluted on a narrowbore (ID: 2 mm) reverse-phase C18 column (MD-150; ESA, Inc., Chelmsford, MA, USA) using MD-TM (ESA, Inc.) mobile phase. A 12-channel CoulArray (ESA, Inc.) equipped with a highly sensitive amperometric microbore cell (model 5041; ESA, Inc.) was used to analyze the content of NE, dopamine, and serotonin with the cell potential set at + 220 mV. The flow rate was set at 0.2 mL/min for all measurements by using a solvent delivery pump (model 585; ESA, Inc.). Peak areas were analyzed using the CoulArray® data analysis software (Chelmsford, MA, USA). All peak areas were within the linear range of the standard curves.

Multiphoton Imaging for Assessment of Vessel Diameter

A custom-built microscope attached to a Tsunami/Millenium laser (10 W; Spectra Physics, Mountain View, CA, USA) and scan box (FV300 Fluoview Software, Olympus, Center Valley, PA, USA) was used for two-photon imaging through a $\times 20$ objective (0.9 NA; Olympus). Fluorescein isothiocyanate-dextran, injected intraarterially, was excited at 825 nm with reflected light detected through a 525/50 filter onto a photomultiplier tube. Pial and penetrating arteries were visualized through an open cranial window and diameters measured using custom-made software (Matlab 2008a software, Mathworks, Natick, MA, USA). Pial vessels were measured at five separate positions each and averaged, while penetrating arteriole measures were obtained from two diameter measures taken perpendicularly to the two elliptical axes. For cortical superfusion experiments, heated artificial cerebral spinal fluid was slowly perfused under the coverslip at $\sim$1 mL/min. Fifteen minutes after atipamezole injection, the artificial cerebral spinal fluid was changed to artificial cerebral spinal fluid containing prazosin (1 μmol/L; Fisher Scientific, Pittsburgh, PA, USA) to assess ability to reverse atipamezole-mediated vasoconstriction.

Intrinsic Optical Signal Imaging

Images were captured at 52 frames per second (348×256) using a 12-bit INFINITY2-1M CCD camera by custom-made software (Matlab 2008a software, Mathworks) resulting in a

pixel size of 9 to 12 μm. To improve signal-to-noise, 10 to 20 15-second trials were averaged for green light responses and 40 to 60 trials for red light responses. Green (570 nm) light is the isosbestic point for hemoglobin resulting in measure of both oxygenated and deoxygenated hemoglobin (total hemoglobin) (Frostig *et al*, 1990). Red (610 nm) light is selective for deoxygenated hemoglobin only (Frostig *et al*, 1990). For further noise reduction, images were averaged temporally to 4 Hz (13 frames averaged) for time series evaluations and 1 Hz (52 frames averaged) for all spatial analyses. Sensory stimulation was initiated after 2 seconds of baseline acquisition. By referencing all frames to the corresponding frame immediately before stimulation, data are expressed as % change from baseline. Spatial analyses were performed on 20% threshold masks of peak blood-flow responses to hindlimb stimulation. The 20% level was chosen to include small parenchymal changes associated with capillary flow, as the largest changes are localized to the large vessels. Increases in blood volume are characterized by a negative reflectance change as more hemoglobin absorbs more (reflects less) 570 nm light.

Hindlimb and Forelimb Stimulation

Stimulation was applied through a pair of 30 gauge needles attached to a photoelectric stimulus isolation unit (PSIU6; Grass Telefactor, West Warwick, RI, USA) connected to a square pulse stimulator (S88K; Grass Telefactor) and controlled by a Master-8 (A.M.P.I.). Sensory stimulation involved the delivery of a 20-pulse train of 0.5 to 2.0 mA/0.5 ms square pulses at 10 Hz. As altering NE levels affects the arousal state of the animal, the stimulus amplitude was titrated in every animal to obtain similar systemic blood pressure responses (<5 mm Hg) to sensory stimulation. Blood pressure waveforms for each trial (10 to 60 trials) of a given experiment were averaged for every animal. Comparing averaged stimulation-evoked blood pressure spikes showed no significant difference between DSP-4 (2.18 ± 0.49 mm Hg; $n=12$), control (1.50 ± 0.35 mm Hg; $n=23$) and atipamezole-treated (3.78 ± 1.21 mm Hg; $n=9$) groups.

Statistical Analysis

All data are expressed as mean values ± standard error mean. Significance was determined using Student's *t*-test (unpaired unless stated otherwise) or analysis of variance using the Holm-Sidak multiple comparison method or analysis of variance on ranks with Dunn's multiple comparison method using Sigmaplot 11.0 software (San Jose, CA, USA).

Results

Enhanced Cortical Norepinephrine is Associated with Decreased Vessel Diameter

The α_2-adrenergic antagonist, atipamezole, and the selective LC neurotoxin DSP-4 have been used extensively to manipulate LC network activity and brain NE concentration. Consistent with previous studies (Fritschy and Grzanna, 1991; Heneka *et al*, 2006), pretreatment of mice with the LC-selective neurotoxin, DSP-4, depleted cortical NE levels by 85% (Table 1). Conversely, as LC neurons possess α_2-adrenergic autoreceptors for feedback inhibition of release (Dennis *et al*, 1987), administering untreated mice the α_2-adrenergic receptor antagonist, atipamezole, augmented baseline cortical NE levels by 30% (Table 1). These manipulations were selective for NE as DSP-4 or atipamezole pretreatment had no effect on cortical serotonin or dopamine levels (Table 1). In addition to the atipamezole effects on basal NE levels reported herein, it is important to note that our previous study showed that an α_2-adrenergic receptor antagonist can further augment NE release in response to salient or noxious stimulation (Bekar *et al*, 2008). Furthermore, tissue samples for high performance liquid chromatography were typically taken from animals after completion of experiments over 1 hour after atipamezole administration when effects had finished peaking and NE levels were returning to baseline (Figure 1). Thus, a 30% increase in basal NE levels with atipamezole treatment is a gross underestimation. Pharmacological treatments showed no significant effects in baseline blood pressure or arterial blood gases (Table 1).

To assess the role of NE in vessel diameter, multiphoton imaging of pial and penetrating arteries was performed before and after administration of the α_2-adrenergic antagonist atipamezole. Consistent with an atipamezole-mediated enhancement of cortical NE (Table 1), pial arteries (46 arteries from 6 animals) and penetrating arterioles (16 arterioles from 8 animals) showed a decrease in diameter that remained for >1 hour after injection (Figure 1). To ensure the α_2-adrenoceptor effects were mediated indirectly via enhanced NE release and not a result of

Table 1 Treatment effects on baseline cortical neuromodulator concentrations, blood pressure, and blood gases

	NE (μmol/L)	*DA (nmol/L)*	*5-HT (nmol/L)*	*BP (mm Hg)*	*pH*	*pCO_2 (mm Hg)*	*pO_2 (mm Hg)*
DSP-4	0.24 ± 0.02* (13)	230 ± 65.6 (13)	10.2 ± 1.85 (13)	85.5 ± 1.57 (12)	7.33 ± 0.01 (13)	35.3 ± 1.64 (13)	97.4 ± 4.85 (13)
Control	1.57 ± 0.09 (4)	141 ± 85.3 (4)	10.1 ± 2.02 (4)	83.3 ± 1.10 (38)	7.34 ± 0.01 (34)	32.6 ± 0.97 (34)	115 ± 3.83 (34)
ati	2.03 ± 0.05* (4)	164 ± 136 (4)	14.4 ± 3.75 (4)	84.8 ± 1.78 (23)	7.29 ± 0.02 (22)	35.9 ± 2.01 (22)	111 ± 5.75 (22)

5-HT, serotonin; ati, atipamezole; BP, blood pressure; DA, dopamine; NE, norepinephrine.
Numbers in parentheses represent the number of animals. *$P < 0.001$ compared with control, Holm-Sidak's test.

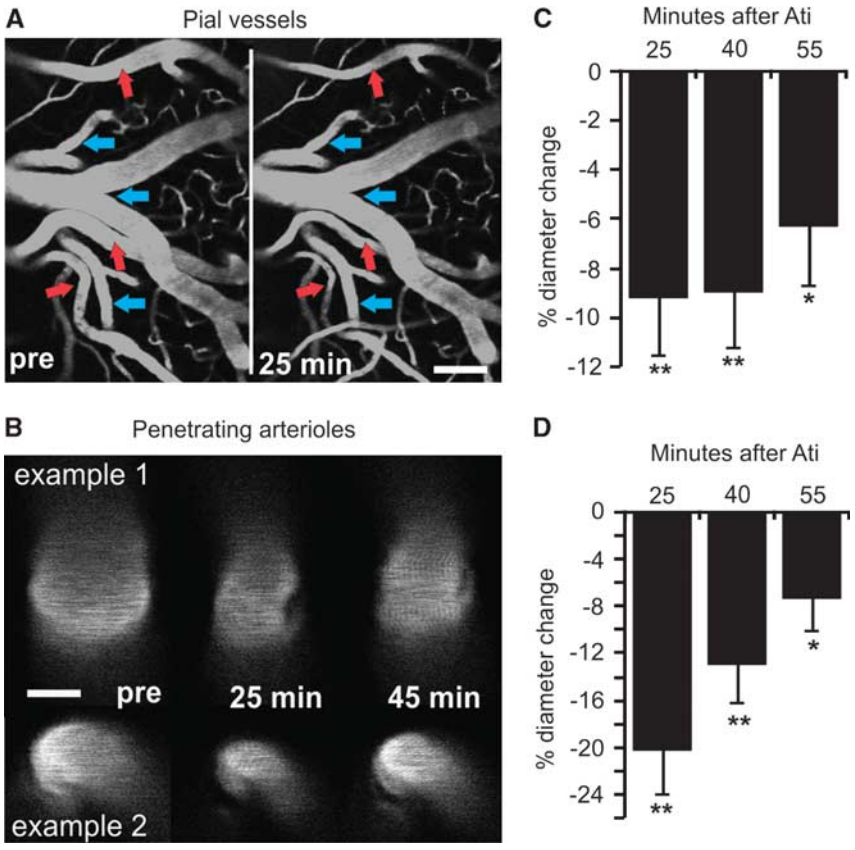

Figure 1 Enhanced cortical norepinephrine (NE) is associated with decreased vessel diameter. (**A**, **B**) Multiphoton images of fluorescein isothiocyanate (FITC)-dextran loaded pial vessels and penetrating arterioles before (pre), 25 and 40 minutes after administration of the $\alpha 2$-adrenergic receptor antagonist atipamezole (ati). Note that surface arteries show constriction (red arrows), whereas veins (blue arrows) do not. Scale bar in (**A**) is 100 μm and in (**B**) 20 μm. (**C**, **D**) Histograms showing % change in vessel diameter at 25, 40, and 55 minutes after atipamezole administration show that the response remains significant for >1 hour. $^{*}P<0.05$, $^{**}P<0.01$, paired *t*-test.

direct disruption of vascular α_2-adrenoceptors, separate experiments were performed where the α_1-adrenergic antagonist, prazosin (1 μmol/L), was superfused across the cortical surface. We found that the diameter of surface arteries constricted from 23.98 ± 2.34 to 17.70 ± 1.48 μm ($P<0.001$) in response to intraperitoneal injection of atipamezole and could be significantly reversed to 21.73 ± 1.76 μm ($P<0.05$; one-way repeated measure analysis of variance; $n=5$) on cortical superfusion with prazosin, indicating that atipamezole increases cortical NE to act via α_1-adrenergic receptors on the cerebral vasculature.

Delayed Locus Coeruleus-Norepinephrine Constriction Enhances Recovery of Functional Hyperemic Responses

Using intrinsic optical imaging of total hemoglobin (570 nm) as a measure of blood (hemoglobin) distribution in mouse somatosensory cortex, we assessed functional blood distribution kinetics across large cortical areas to understand the role of LC-NE network-mediated vasoconstriction in functional hyperemia. We use the terms blood distribution or blood volume to describe alterations in blood flow because intrinsic imaging of hemoglobin tracks changes in red blood cell number and does not necessarily reflect changes in blood supply *per se*. We found that the LC-NE neuromodulatory network counteracts the hyperemic response to sensory stimulation (Figure 2). To investigate temporal aspects of blood distribution dynamics, average reflectance of 500 μm diameter regions in both forelimb and stimulated hindlimb somatosensory cortex were measured; a negative reflectance indicates an increase in blood volume. Consistent with prior studies, hindlimb stimulation increased blood distribution in hindlimb cortex concomitantly with a decrease in the forelimb region (Figure 2). Notably, the duration of the hindlimb hyperemic response is significantly shortened with enhanced NE (atipamezole treated), and lengthened in NE-deficient mice (DSP-4 treated) (Figures 2B and 2C). The LC-mediated effect on the duration of hyperemia is consistent with the significant ability of NE to constrict the vasculature (Figure 1). Hindlimb stimulation results in phasic discharge of LC neurons, causing global NE release that is delayed relative to the sensory-evoked hindlimb blood volume increase. As such, the NE-mediated constriction

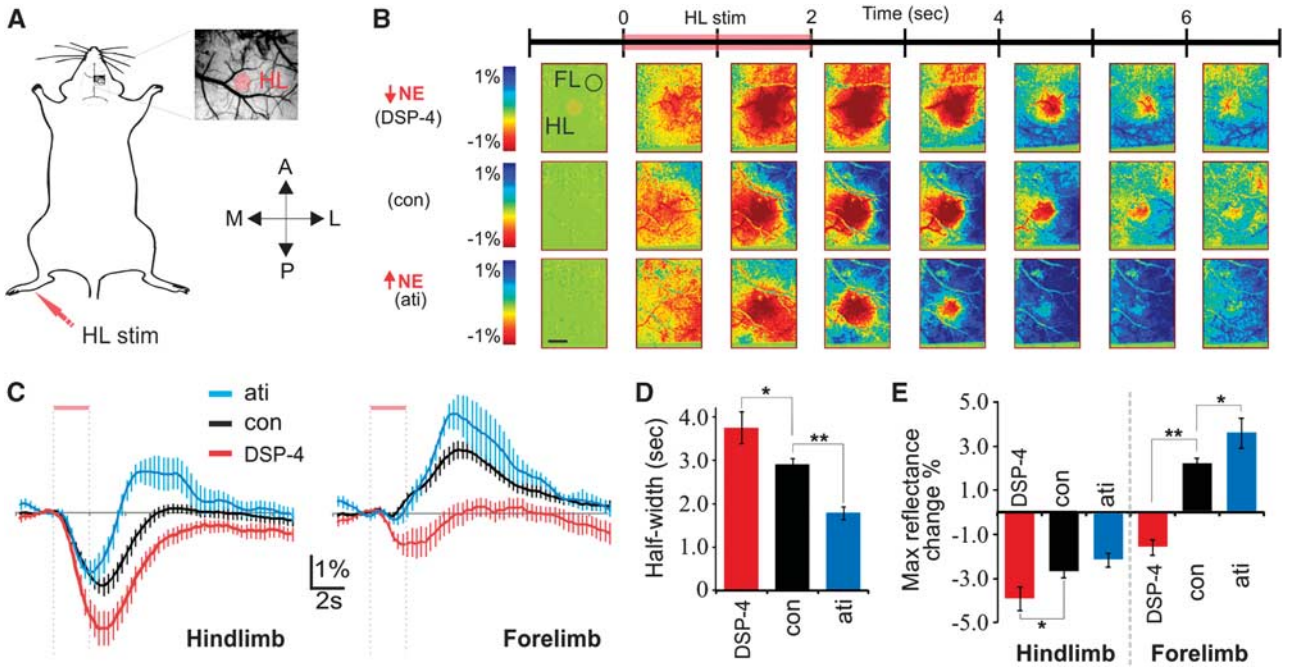

Figure 2 Characterization of norepinephrine (NE)-mediated effects on temporal dynamics of the blood distribution response to hindlimb stimulation. (**A**) Schematic of animal preparation with thin skull cranial window and limb stimulation. (**B**) Intrinsic imaging of total hemoglobin (570 nm) in response to hindlimb stimulation showing response in a cortical NE-depleted (top), nontreated (middle), and NE release-enhanced mouse (bottom) for comparison. The seven image sequences illustrate 1 second bins before and after stimulation normalized to the 1 second bin before stimulation. A, anterior; ati, atipamezole; con, control; FL, forelimb; HL, hindlimb; L, lateral; M, medial; P, posterior; stim, stimulation. Scale bar is 1 mm. (**C**) Average intensity over 15 seconds in hindlimb and forelimb regions for the different treatment groups (control, $n = 24$; DSP-4, $n = 15$; atipamezole, $n = 9$). (**D**) Histogram comparing full widths at half maximal hindlimb hyperemic responses shown in (**C**) (Holm-Sidak test, $*P < 0.05$, $**P < 0.01$). (**E**) Comparison of maximal changes in light reflectance after hindlimb stimulation (Holm-Sidak test, $*P < 0.05$, $**P < 0.01$).

serves to counter blood-flow increases and results in a hyperemic response that more closely matches the temporal aspects of the stimulation (Figures 2B and 2C). The fact that sensory-evoked hyperemia extends beyond the stimulated brain region in NE-deficient mice (Figures 2B–2D) but not in control mice suggests that active vasoconstrictors are necessary for focusing blood distribution in functional hyperemia.

The Locus Coeruleus-Norepinephrine Network Focuses Blood Volume Changes to Region of Oxygen Demand

Assessment of global blood distribution dynamics using optical imaging shows that spatial characteristics of neurovascular coupling is highly dependent on the LC-NE network (Figure 3). In contrast to single point laser Doppler measures, intrinsic optical imaging enables analysis of global distribution dynamics. Analysis of 500 μm diameter regions within the peak response shows the importance of NE in temporal changes (similar to laser Doppler), but grossly underestimates effects on global dynamics (see spatial differences in Figure 3A). In attempt to incorporate both spatial and temporal components of the response, we applied 20% threshold masks to each of three 1-second time bins (from 1 to 4 seconds after stimulation) and summed the pixel intensities (area and amplitude information) of all three as a measure of blood volume change (Figures 3A and 3B). NE-deficient animals showed significantly larger, whereas NE-enhanced animals showed more restricted blood volume increases relative to controls (Figure 3B). Comparison of hindlimb optical responses measuring the initial increase in reduced hemoglobin (610 nm; 'dip', measure of oxygen demand) versus total hemoglobin (570 nm; measure of blood volume) enables a basic assessment of metabolic coupling (Figures 3C and 3D). The initial 'dip' is commonly used to localize the region of neural activity (Frostig *et al*, 1990; Winship *et al*, 2007). Although pretreatment of mice with DSP-4 (low NE) does not alter oxygen demand as measured by the increase in reduced hemoglobin (Figure 3D, top), the disparity between blood volume and demand was increased more than sixfold compared with nontreated mice (Figure 3D, bottom). Thus, in addition to the temporal synchronization shown in Figure 1, NE spatially focuses the hindlimb hyperemic response to more precisely reflect oxygen demand. In other words, NE-deficient animals exhibited hyperemic responses that included large surrounding regions, whereas the hyperemia in NE-enhanced

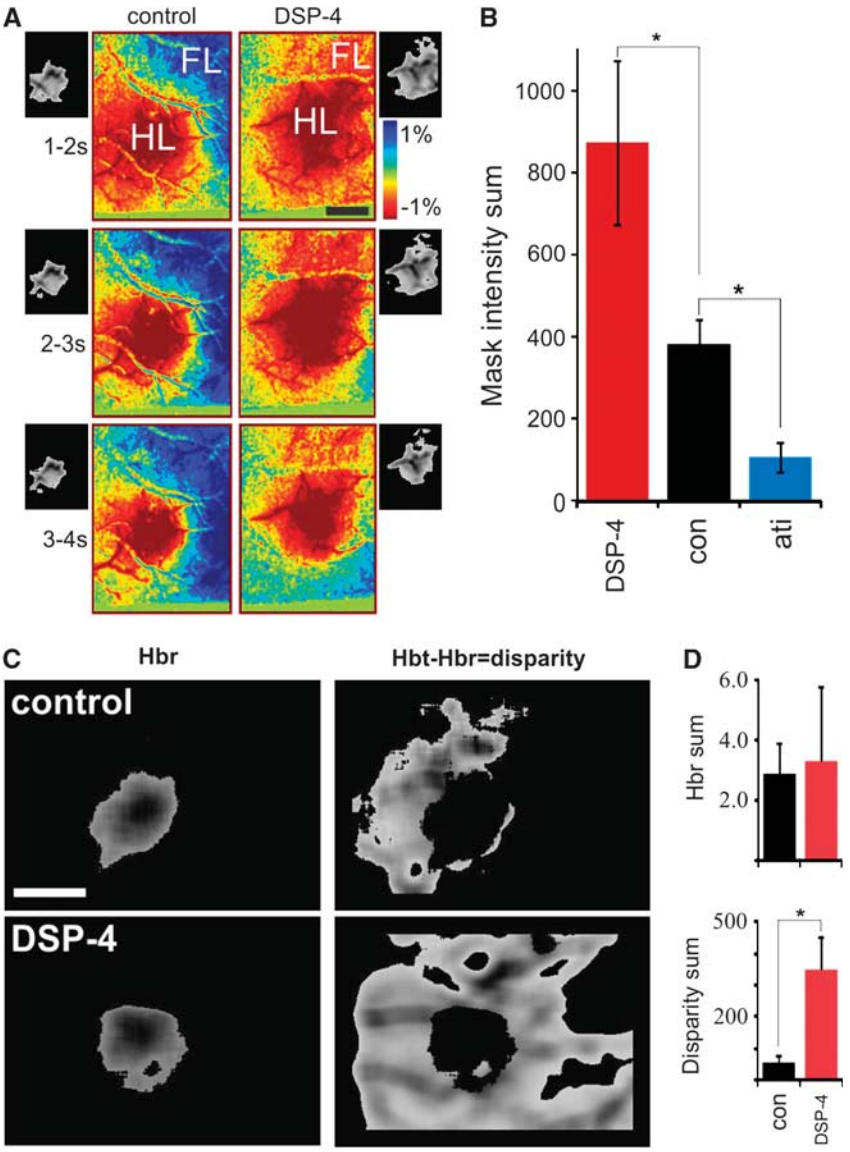

Figure 3 The locus coeruleus decreases blood distribution to optimize neurovascular coupling. (**A**) Optical imaging for spatial assessment of the blood distribution response to hindlimb stimulation. Corresponding 20% peak threshold masks are attached. (**B**) Combined temporal and spatial aspects of drug effects determined by summing pixel intensities of the three 1-second 20% threshold masks 1 to 4 seconds after stimulation (control, $n = 24$; DSP-4, $n = 15$; atipamezole, $n = 9$; Dunn's test, $^*P < 0.05$). (**C**) 20% threshold mask of reduced (left, 610 nm), and total (570 nm) minus reduced (right) hemoglobin response. Hbr, reduced hemoglobin; Hbt, total hemoglobin. (**D**) Quantifying Hbt 20% threshold mask pixels outside the corresponding Hbr threshold mask gives a measure of metabolism-flow disparity. Hbr volumes show no difference (top) whereas Hbt-Hbr volumes are significantly different (bottom) (DSP-4, $n = 7$; control, $n = 8$; *t*-test, $P = 0.003$). Scale bars in (**A**) and (**C**) are 1 mm. FL, forelimb; HL, hindlimb.

animals was restricted to the stimulated region (hindlimb cortex) only.

The Norepinephrine-Mediated Vasoconstriction Enables Rapid Redistribution of Blood

In addition to focusing blood distribution increases to areas of oxygen demand, NE-mediated global vasoconstriction serves to enhance temporal synchronization of cerebral blood volume to the ever shifting activity pattern of the awake brain. Theoretically, if all resistance vessels were maximally dilated, then local vasodilatory signals would be unable to redistribute flow. In practice, a global decrease in vessel diameter (NE-mediated vasoconstriction) would actively force flow along the path of least resistance (local vasodilatation), resulting in faster redistribution of blood for better synchronization with oxygen demand.

To assess the role of LC-NE in blood volume redistribution, the same imaging paradigm as above was used, this time adding a forelimb stimulation immediately after the hindlimb stimulation

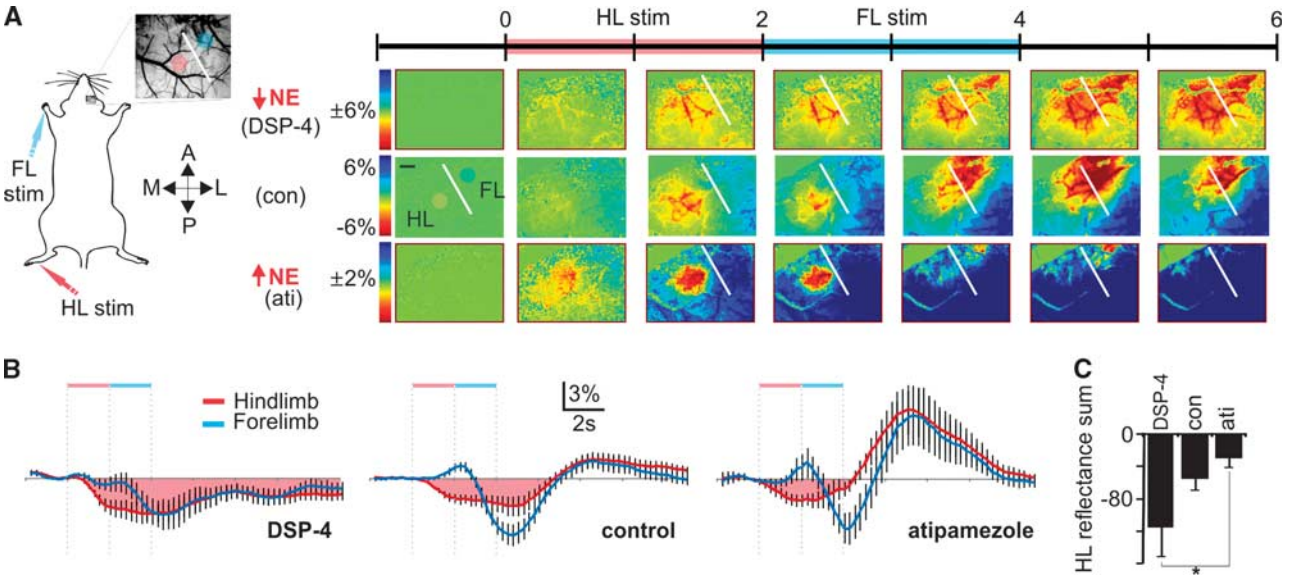

Figure 4 The locus coeruleus-mediated decrease in vessel diameter enables rapid redistribution of red blood cells. (**A**) Intrinsic imaging of total hemoglobin in response to hindlimb stimulation (HLS) followed by forelimb stimulation (FLS) showing responses in a cortical norepinephrine (NE)-depleted (top), nontreated (middle), and NE release-enhanced mouse (bottom) for comparison. Scale bar is 500 μm. (**B**) Average intensity over 15 seconds in hindlimb and forelimb regions. Note the HLS-evoked decrease in blood volume in the forelimb region immediately before being overridden by an FLS-mediated blood distribution increase in the control and atipamezole groups. (DSP-4, $n = 5$; control, $n = 9$; atipamezole, $n = 5$). (**C**) The blood distribution increase in the HL region is prolonged in NE-depleted animals (Holm-Sidak test, $P = 0.01$). Reflectance sum is the temporal sum of the % change in reflectance after hindlimb stimulation as shown by the pink shaded area in (**B**).

(Figure 4A). Under conditions of low cortical NE, the hindlimb blood-flow increase is prolonged despite subsequent forelimb stimulation (Figures 4A–4C). In contrast, hindlimb flow recovers coincident with forelimb hyperemia under conditions of enhanced NE release (Figures 4A–4C). This is consistent with the NE-mediated optimization of the coupling of blood volume with oxygen demand shown in Figures 2 and 3. Comparison of forelimb hyperemic responses alone or after hindlimb stimulation (which is associated with LC-mediated evoked NE release) enables evaluation of the rate of blood redistribution with or without NE-mediated preconstriction. Forelimb hyperemic responses show faster increases (steeper slope) when coupled with hindlimb stimulation-evoked NE-mediated vasoconstriction (Figure 5). Although LC-mediated global NE release results in global constriction (Raichle *et al*, 1975), neural activity can override it (Peppiatt *et al*, 2006) to generate a blood volume increase, as seen in control and atipamezole treatment groups (Figure 4B). Such a global constriction with local dilation would enhance the rerouting of local blood supply. Thus, the LC-NE network optimizes global coordination of blood distribution with oxygen demand.

Discussion

These studies are the first to provide a physiological context for the commonly observed NE-mediated vasoconstriction. Prior studies assessing regulatory mechanisms in blood flow are largely based on deeply anesthetized animal models in which LC contributions would be concealed. Furthermore, only by imaging large areas of cortex using intrinsic optical imaging can one appreciate the global aspects of the LC-NE neuromodulatory network on blood distribution kinetics in response to single and multiple stimulation paradigms. By manipulating cortical NE output using the selective LC neurotoxin DSP-4 (Fritschy and Grzanna, 1991) or inhibiting LC auto-feedback inhibition with the α_2-adrenergic antagonist atipamezole (Bekar *et al*, 2008; Dennis *et al*, 1987), we were able to assess the role of NE in functional blood distribution kinetics. First, we show that the α_2-adrenergic antagonist atipamezole results in decreased vessel diameter (Figure 1) via α_1-adrenergic receptors. We then show that the NE-mediated decrease in vessel diameter improves synchronization of both temporal (Figure 2) and spatial (Figures 3A and 3B) characteristics of the sensory stimulation-mediated hyperemia and surround blood volume decrease. These effects are consistent with the idea that LC-NE enhances coupling of blood distribution changes with local oxygen demands (Figures 3C and 3D) and improves the ability to quickly redistribute blood to subsequently active brain regions (Figure 4). Thus, the NE-mediated global vasoconstriction enhances the temporal (Figures 5A and 5B) and spatial (Figures 3 and 5C) specificity of the hyperemic response, consistent with a constriction-mediated enhancement of surround blood volume decreases.

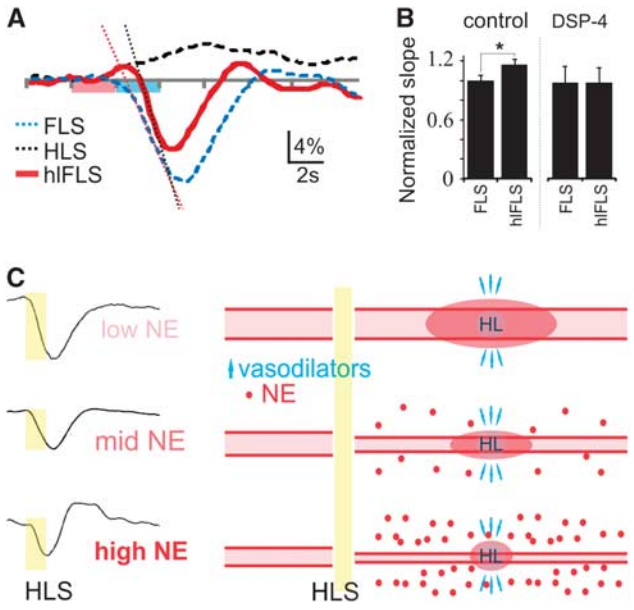

Figure 5 The locus coeruleus affects rate of blood redistribution. (**A**) Forelimb region responses (570 nm) to hindlimb (HLS), forelimb (FLS), and combined hindlimb-forelimb stimulation (hlFLS). (**B**) The slope of the FLS-mediated blood distribution increase is greater after HLS (with associated norepinephrine (NE)-mediated constriction) compared with FLS alone (paired *t*-test, $P = 0.03$). (**C**) Schematic summarizing the proposed impact of NE on the sensory hyperemic response. On the left are the average blood distribution responses to HLS from Figure 2C representing low NE (DSP-4), mid NE (con) and high NE (ati). They show the NE-mediated effects on the temporal aspects of the hyperemia. On the right are the corresponding pictorials of single blood vessels representing the vascular tree spanning the somatosensory cortex, before and after HLS. Under low NE conditions (lowest baseline vascular tone), HLS leads to release of local vasodilators with an increase in blood flow and limited corresponding constriction or redirection of blood flow in the surrounding cortex. Under high NE conditions, HLS releases vasodilators with subsequent global NE release to constrict the vasculature and spatially and temporally synchronize the hyperemic response with the active HL region.

The α_2-adrenergic antagonist, atipamezole, and the selective LC neurotoxin DSP-4 have been used extensively to manipulate LC-NE network activity/function. The α_2-adrenergic antagonist, atipamezole, has been used to enhance LC function for improved cognitive performance in both normal and aged (Haapalinna *et al*, 2000) rats making it a strong candidate for potential therapeutic applications in neurodegenerative diseases (Pertovaara *et al*, 2005). Additional studies using the α_2-adrenergic antagonist dexefaroxan (Debeir *et al*, 2004) support the idea that pharmacologically enhancing NE release may prove both therapeutic and protective in neurodegenerative disease progression (Marien *et al*, 2004). As far as noninvasive pharmacological approaches for depletion or destruction of the LC-NE network goes, DSP-4 has been shown to be the most selective for LC noradrenergic projection areas, leaving noradrenergic neurons of the A1 and A2 regions intact (Fritschy and Grzanna, 1989, 1991). Although some controversy surrounding the effectiveness of a single dose of DSP-4 for depleting/destroying LC pathways exists that may depend partially on species differences (Szot *et al*, 2010), many studies using two injections separated by 1 week (as used in the current study) have shown dramatic reductions in LC numbers and NE concentrations throughout LC projection areas (Bekar *et al*, 2008; Heneka *et al*, 2002, 2006). Given the effects on cortical NE levels (by high performance liquid chromatography, Table 1) and pial vessel diameter (Figure 1), the present pharmacological models provide a suitable backdrop with which to evaluate the role of the LC-NE network in functional blood distribution kinetics.

The LC-mediated vasoconstriction likely occurs simultaneously at many levels of the vascular tree. Although early studies suggest NE-mediated regulation of cortical blood flow derives from superior cervical ganglion projections to pial vessels and penetrating arterioles (Gotoh *et al*, 1986), later analysis showed that LC projections are closely associated with cerebral arterioles and capillaries (Cohen *et al*, 1997) and also directly affect blood flow (Ohta *et al*, 1991; Raichle *et al*, 1975). Ultrastructural analysis suggests that LC neurons do not directly innervate vessels but rather form varicosities in the paravascular space adjacent to arterioles and capillaries (Cohen *et al*, 1997). Thus, NE may act on cells associated with the vasculature rather than directly mediating constriction of vascular smooth muscle cells. Functional studies have supported this conclusion by showing that NE mediates vasoconstriction in slice preparations through actions on astrocytes (Mulligan and MacVicar, 2004), pericytes (Peppiatt *et al*, 2006), and to a lesser extent on isolated penetrating arterioles (Dacey and Duling, 1984). Thus, LC neurons constitute an ideal conduit for global sympathetic regulation of the vasculature.

As fluid (blood) passively flows through a network of vessels taking the path of least resistance, distribution is dependent on local and distant mediators of vessel diameter. Local vessel dilation will increase fluid volume at the expense of volume loss in neighboring vessels, a concept known as 'steal'. The most efficient means to redirect fluid distribution is to dilate one vessel and constrict another. This concept underlies the significance of both dilation and constriction in functional hyperemia. The balance between vasoconstrictors (global?) and vasodilators (local activity) dictates vessel diameter and blood-flow distribution. By decreasing vessel diameter nonselectively (Figure 1; Raichle *et al*, 1975), NE spatially and temporally optimizes redistribution to areas where vasodilatory signals overpower NE-mediated vasoconstriction (Figure 4B; Peppiatt *et al*, 2006). This does not only apply to activity-dependent processes, however. Basal vascular tone, which would be correlated with the extent of arousal and thus LC output, is known to

affect the temporal dynamics of functional hyperemic responses (Cohen *et al*, 2002), emphasizing the importance of a system that can rapidly change global vascular tone.

The significance of a nonselective NE-mediated optimization in blood distribution kinetics is that it may also refine/optimize other vascular regulatory mechanisms. Metabolic factors such as the NADH/NAD+ (Vlassenko *et al*, 2006) and lactate/pyruvate (Gordon *et al*, 2008; Mintun *et al*, 2004) ratios as well as the neurogenic vasoactive factors including arachidonic acid metabolites (Gordon *et al*, 2008), potassium (Dunn and Nelson, 2010), nitric oxide (Liu *et al*, 2008), and CO (Li *et al*, 2008) can all be integrated locally to determine regional vessel diameter for passive distribution of blood on a backdrop of NE-mediated global constriction (Figure 5C). Norepinephrine has also been shown to enhance surround inhibition through GABAergic interneurons (Lei *et al*, 2007), supporting the possible involvement of interneuron-derived dilatory or constrictive peptides (Cauli *et al*, 2004; Vaucher *et al*, 2000). Furthermore, consistent with peripheral catecholamine effects, an NE-mediated glycogenolysis and increase in glycolysis (Hertz *et al*, 2004) could maintain the metabolic state of relatively inactive tissue. Norepinephrine-mediated influence of the NADH/NAD+ and lactate/pyruvate ratios with subsequent effects on prostaglandin release (Gordon *et al*, 2008) may also shift the balance of factors that dictate net vasodilation versus vasoconstriction to better define regions of highest oxygen demand. Thus, NE's role as a neuromodulator seemingly extends to modulation/optimization of coupling oxygen delivery to oxygen demand.

Given that blood-flow responses to sensory stimulation are typically larger (2 to 4 times) than the change in cerebral metabolic rate of oxygen (Buxton, 2010) and that oxygen-extraction decreases during activity-dependent increases in blood flow (Fox and Raichle, 1986), the temporally and spatially reduced NE-mediated hyperemia observed here (Figures 2 and 3) is consistent with an optimized use of limited oxygen availability. The global release of NE by LC activity provides a homogeneous enhancement in vasoconstrictive tone that is balanced by local activity-generated vasodilators resulting in a more precise control of the blood distribution response. The LC-NE effects are delayed relative to the stimulus onset (Hirata and Aston-Jones, 1994; Nieuwenhuis *et al*, 2005) and thus are important for curtailing/reducing the hyperemic response and speeding redistribution to subsequent brain activity. In the context of enhanced arousal with increased tonic LC activity and many active brain regions, the increased vasoconstrictive tone would serve a long-term function to counterbalance local dilatory effects and blunt neurovascular responses to prevent over- and undershooting metabolic requirements. Taking into account that NE-mediated glycogenolysis and enhanced glycolysis (Hertz *et al*, 2004) can help reduce energy deficits, increased LC activity would minimize the effect of any decreases in oxygen availability.

The NE-mediated blood-flow decrease may also help explain the commonly observed negative blood oxygenation level-dependent functional magnetic resonance imaging signal. The surround inhibition of neural activity is a common phenomenon involving inhibitory interneurons (Boorman *et al*, 2010; Devor *et al*, 2007) with at least one subset of interneuron containing vasoconstrictor peptides (Cauli *et al*, 2004). This enables an inherent activity-dependent redistribution of blood from surround to the center active region. It is in this regard that NE has been shown to enhance surround inhibition through GABAergic interneurons (Lei *et al*, 2007) while stimulating anaerobic metabolic processes (Hertz *et al*, 2004) and shifting the balance between vasodilation and vasoconstriction in favor of constriction. Thus, although not solely responsible for the negative blood oxygenation level-dependent functional magnetic resonance imaging phenomenon, NE from the LC may contribute.

As outlined in this study, the LC-NE network mirrors the functionality of the peripheral sympathetic nervous system and provides a global framework in which to incorporate all blood-flow regulatory mechanisms. The large disparity between blood volume and oxygen demand and the decreased ability to redistribute blood under NE-deficient conditions may render subsequently active regions subject to mild transient hypoxic episodes. Furthermore, the ability for NE to enhance temporal coupling between oxygen demand and supply suggests that under conditions of LC neuron loss like that associated with Alzheimer and Parkinson diseases (Marien *et al*, 2004), the hyperemic response may be delayed and hypoxia-reperfusion-like mini injuries may result. Accumulation of such events over time may promote ischemic damage and hasten disease progression. In light of a known decline in LC neuron number and cortical NE levels with age (Marcyniuk *et al*, 1989) and Alzheimer's disease (Marcyniuk *et al*, 1986; Zarow *et al*, 2003), and that neurovascular dysregulation is an early indicator of pathologic assessment (Iadecola, 2004; Zlokovic, 2011), understanding the role of the LC-NE network in neurovascular regulation will be important for the future design of therapeutic strategies for slowing the cognitive decline associated with aging or disease.

Acknowledgements

The authors thank C Iadecola, K Kasischke, M Lauritzen, L Park, and T Takano for comments on the manuscript. The authors also thank W Peng and H Kang for help with surgical preparations and P Rappold and K Tieu for help with HPLC.

Disclosure/conflict of interest

The authors declare no conflict of interest.

References

Bekar LK, He W, Nedergaard M (2008) Locus coeruleus alpha-adrenergic-mediated activation of cortical astrocytes *in vivo*. *Cereb Cortex* 18:2789–95

Berridge CW, Waterhouse BD (2003) The locus coeruleus-noradrenergic system: modulation of behavioral state and state-dependent cognitive processes. *Brain Res Brain Res Rev* 42:33–84

Boorman L, Kennerley AJ, Johnston D, Jones M, Zheng Y, Redgrave P, Berwick J (2010) Negative blood oxygen level dependence in the rat: a model for investigating the role of suppression in neurovascular coupling. *J Neurosci* 30:4285–94

Buxton RB (2010) Interpreting oxygenation-based neuroimaging signals: the importance and the challenge of understanding brain oxygen metabolism. *Front Neuroenergetics* 2:8

Cauli B, Tong XK, Rancillac A, Serluca N, Lambolez B, Rossier J, Hamel E (2004) Cortical GABA interneurons in neurovascular coupling: relays for subcortical vasoactive pathways. *J Neurosci* 24:8940–9

Cohen ER, Ugurbil K, Kim SG (2002) Effect of basal conditions on the magnitude and dynamics of the blood oxygenation level-dependent fMRI response. *J Cereb Blood Flow Metab* 22:1042–53

Cohen Z, Molinatti G, Hamel E (1997) Astroglial and vascular interactions of noradrenaline terminals in the rat cerebral cortex. *J Cereb Blood Flow Metab* 17: 894–904

Dacey Jr RG, Duling BR (1984) Effect of norepinephrine on penetrating arterioles of rat cerebral cortex. *Am J Physiol* 246:H380–5

Debeir T, Marien M, Ferrario J, Rizk P, Prigent A, Colpaert F, Raisman-Vozari R (2004) *In vivo* upregulation of endogenous NGF in the rat brain by the alpha2-adrenoreceptor antagonist dexefaroxan: potential role in the protection of the basalocortical cholinergic system during neurodegeneration. *Exp Neurol* 190: 384–95

Dennis T, L'Heureux R, Carter C, Scatton B (1987) Presynaptic alpha-2 adrenoceptors play a major role in the effects of idazoxan on cortical noradrenaline release (as measured by *in vivo* dialysis) in the rat. *J Pharmacol Exp Ther* 241:642–9

Devor A, Hillman EM, Tian P, Waeber C, Teng IC, Ruvinskaya L, Shalinsky MH, Zhu H, Haslinger RH, Narayanan SN, Ulbert I, Dunn AK, Lo EH, Rosen BR, Dale AM, Kleinfeld D, Boas DA (2008) Stimulus-induced changes in blood flow and 2-deoxyglucose uptake dissociate in ipsilateral somatosensory cortex. *J Neurosci* 28:14347–57

Devor A, Tian P, Nishimura N, Teng IC, Hillman EM, Narayanan SN, Ulbert I, Boas DA, Kleinfeld D, Dale AM (2007) Suppressed neuronal activity and concurrent arteriolar vasoconstriction may explain negative blood oxygenation level-dependent signal. *J Neurosci* 27: 4452–9

Dunn KM, Nelson MT (2010) Potassium channels and neurovascular coupling. *Circ J* 74:608–16

Fox PT, Raichle ME (1986) Focal physiological uncoupling of cerebral blood flow and oxidative metabolism during somatosensory stimulation in human subjects. *Proc Natl Acad Sci USA* 83:1140–4

Fritschy JM, Grzanna R (1989) Immunohistochemical analysis of the neurotoxic effects of DSP-4 identifies two populations of noradrenergic axon terminals. *Neuroscience* 30:181–97

Fritschy JM, Grzanna R (1991) Selective effects of DSP-4 on locus coeruleus axons: are there pharmacologically different types of noradrenergic axons in the central nervous system? *Prog Brain Res* 88:257–68

Frostig RD, Lieke EE, Ts'o DY, Grinvald A (1990) Cortical functional architecture and local coupling between neuronal activity and the microcirculation revealed by *in vivo* high-resolution optical imaging of intrinsic signals. *Proc Natl Acad Sci USA* 87:6082–6

Gordon GR, Choi HB, Rungta RL, Ellis-Davies GC, MacVicar BA (2008) Brain metabolism dictates the polarity of astrocyte control over arterioles. *Nature* 456:745–9

Gotoh F, Fukuuchi Y, Amano T, Tanaka K, Uematsu D, Suzuki N, Kobari M, Obara K (1986) Comparison between pial and intraparenchymal vascular responses to cervical sympathetic stimulation in cats. Part 1. Under normal resting conditions. *J Cereb Blood Flow Metab* 6:342–7

Haapalinna A, Sirvio J, MacDonald E, Virtanen R, Heinonen E (2000) The effects of a specific alpha(2)-adrenoceptor antagonist, atipamezole, on cognitive performance and brain neurochemistry in aged Fisher 344 rats. *Eur J Pharmacol* 387:141–50

Harel N, Lee SP, Nagaoka T, Kim DS, Kim SG (2002) Origin of negative blood oxygenation level-dependent fMRI signals. *J Cereb Blood Flow Metab* 22:908–17

Heneka MT, Galea E, Gavriluyk V, Dumitrescu-Ozimek L, Daeschner J, O'Banion MK, Weinberg G, Klockgether T, Feinstein DL (2002) Noradrenergic depletion potentiates beta-amyloid-induced cortical inflammation: implications for Alzheimer's disease. *J Neurosci* 22: 2434–42

Heneka MT, Ramanathan M, Jacobs AH, Dumitrescu-Ozimek L, Bilkei-Gorzo A, Debeir T, Sastre M, Galldiks N, Zimmer A, Hoehn M, Heiss WD, Klockgether T, Staufenbiel M (2006) Locus ceruleus degeneration promotes Alzheimer pathogenesis in amyloid precursor protein 23 transgenic mice. *J Neurosci* 26:1343–54

Hertz L, Chen Y, Gibbs ME, Zang P, Peng L (2004) Astrocytic adrenoceptors: a major drug target in neurological and psychiatric disorders? *Curr Drug Targets CNS Neurol Disord* 3:239–67

Hirata H, Aston-Jones G (1994) A novel long-latency response of locus coeruleus neurons to noxious stimuli: mediation by peripheral C-fibers. *J Neurophysiol* 71: 1752–61

Iadecola C (2004) Neurovascular regulation in the normal brain and in Alzheimer's disease. *Nat Rev Neurosci* 5: 347–60

Lei S, Deng PY, Porter JE, Shin HS (2007) Adrenergic facilitation of GABAergic transmission in rat entorhinal cortex. *J Neurophysiol* 98:2868–77

Li A, Xi Q, Umstot ES, Bellner L, Schwartzman ML, Jaggar JH, Leffler CW (2008) Astrocyte-derived CO is a diffusible messenger that mediates glutamate-induced cerebral arteriolar dilation by activating smooth muscle cell KCa channels. *Circ Res* 102:234–41

Liu X, Li C, Falck JR, Roman RJ, Harder DR, Koehler RC (2008) Interaction of nitric oxide, 20-HETE, and EETs during functional hyperemia in whisker

barrel cortex. *Am J Physiol Heart Circ Physiol* 295:H619–31
Logothetis NK (2007) The ins and outs of fMRI signals. *Nat Neurosci* 10:1230–2
Marcyniuk B, Mann DM, Yates PO (1986) The topography of cell loss from locus caeruleus in Alzheimer's disease. *J Neurol Sci* 76:335–45
Marcyniuk B, Mann DM, Yates PO (1989) The topography of nerve cell loss from the locus caeruleus in elderly persons. *Neurobiol Aging* 10:5–9
Marien MR, Colpaert FC, Rosenquist AC (2004) Noradrenergic mechanisms in neurodegenerative diseases: a theory. *Brain Res Brain Res Rev* 45:38–78
Mintun MA, Vlassenko AG, Rundle MM, Raichle ME (2004) Increased lactate/pyruvate ratio augments blood flow in physiologically activated human brain. *Proc Natl Acad Sci USA* 101:659–64
Mulligan SJ, MacVicar BA (2004) Calcium transients in astrocyte endfeet cause cerebrovascular constrictions. *Nature* 431:195–9
Nieuwenhuis S, Aston-Jones G, Cohen JD (2005) Decision making, the P3, and the locus coeruleus-norepinephrine system. *Psychol Bull* 131:510–32
Ohta K, Gotoh F, Shimazu K, Amano T, Komatsumoto S, Hamada J, Takahashi S (1991) Locus coeruleus stimulation exerts different influences on the dynamic changes of cerebral pial and intraparenchymal vessels. *Neurol Res* 13:164–7
Peppiatt CM, Howarth C, Mobbs P, Attwell D (2006) Bidirectional control of CNS capillary diameter by pericytes. *Nature* 443:700–4
Pertovaara A, Haapalinna A, Sirvio J, Virtanen R (2005) Pharmacological properties, central nervous system effects, and potential therapeutic applications of atipamezole, a selective alpha2-adrenoceptor antagonist. *CNS Drug Rev* 11:273–88
Raichle ME, Hartman BK, Eichling JO, Sharpe LG (1975) Central noradrenergic regulation of cerebral blood flow and vascular permeability. *Proc Natl Acad Sci USA* 72:3726–30
Raichle ME, Mintun MA (2006) Brain work and brain imaging. *Annu Rev Neurosci* 29:449–76
Shih YY, Chen CC, Shyu BC, Lin ZJ, Chiang YC, Jaw FS, Chen YY, Chang C (2009) A new scenario for negative functional magnetic resonance imaging signals: endogenous neurotransmission. *J Neurosci* 29: 3036–44
Shmuel A, Augath M, Oeltermann A, Logothetis NK (2006) Negative functional MRI response correlates with decreases in neuronal activity in monkey visual area V1. *Nat Neurosci* 9:569–77
Szot P, Miguelez C, White SS, Franklin A, Sikkema C, Wilkinson CW, Ugedo L, Raskind MA (2010) A comprehensive analysis of the effect of DSP4 on the locus coeruleus noradrenergic system in the rat. *Neuroscience* 166:279–91
Vaucher E, Tong XK, Cholet N, Lantin S, Hamel E (2000) GABA neurons provide a rich input to microvessels but not nitric oxide neurons in the rat cerebral cortex: a means for direct regulation of local cerebral blood flow. *J Comp Neurol* 421:161–71
Vlassenko AG, Rundle MM, Raichle ME, Mintun MA (2006) Regulation of blood flow in activated human brain by cytosolic NADH/NAD+ ratio. *Proc Natl Acad Sci USA* 103:1964–9
Winship IR, Plaa N, Murphy TH (2007) Rapid astrocyte calcium signals correlate with neuronal activity and onset of the hemodynamic response *in vivo*. *J Neurosci* 27:6268–72
Zarow C, Lyness SA, Mortimer JA, Chui HC (2003) Neuronal loss is greater in the locus coeruleus than nucleus basalis and substantia nigra in Alzheimer and Parkinson diseases. *Arch Neurol* 60:337–41
Zlokovic BV (2011) Neurovascular pathways to neurodegeneration in Alzheimer's disease and other disorders. *Nat Rev Neurosci* 12:723–38